Using a melanin granule lattice model to study the thermal effects of pulsed and scanning light irradiations through a measurement aperture

Do-Hyun Kim

Using a melanin granule lattice model to study the thermal effects of pulsed and scanning light irradiations through a measurement aperture

Do-Hyun Kim
U.S. Food and Drug Administration, Center for Devices and Radiological Health, 10903 New Hampshire Avenue,
Silver Spring, Maryland 20993

Abstract. Optical radiation hazards of scanning light sources are often evaluated using pulsed light source criteria, with the relevant pulse parameter equivalent to the scanning light source determined by the energy delivered through a measurement aperture. However, physical equivalence has not been completely understood: a pulsed light source is temporally dynamic but spatially stationary, while a scanning light source is temporally stationary but spatially dynamic. This study introduces a numerical analysis based upon the melanin granule lattice model to investigate the equivalence of scanning and pulsed light sources through a measurement aperture and their respective thermal effects in the pigmented retinal layer. The numerical analysis calculates the thermal contribution of individual melanin granules with varying temporal sequence, and finds that temperature changes and thermal damage thresholds for the two different types of light sources were not equal. However, dwell times of 40 to 200 μsec did not produce significant differences between pulsed and scanning light sources in temperature change and thermal damage thresholds to the sample tissue. © *2011 Society of Photo-Optical Instrumentation Engineers (SPIE).*
[DOI: 10.1117/1.3656746]

Keywords: laser safety; eye protection; optical standards; photothermal effects; scanning laser; pulsed laser; melanin granule model.

Paper 11242RR received May 16, 2011; revised manuscript received Sep. 10, 2011; accepted for publication Oct. 10, 2011; published online Nov. 22, 2011.

1 Introduction

A large portion of optical medical devices are based upon scanning technology; however, a proper method to evaluate scanning (or scanned) devices for their optical radiation hazard is not completely established. Commonly used guidances suggest evaluating scanning light sources using pulsed source criteria. For example, according to ISO 15004-2,[1] scanning instruments shall be evaluated using the pulsed instrument criteria when the scan lengths are greater than the diameter of the measurement aperture; scanning laser radiation is defined as laser radiation having a time-varying direction, origin, or pattern of propagation with respect to a stationary frame of reference. It is a reasonable approach, since scanning light appears in the measurement aperture and then disappears after a certain dwell-time, thus resembling the on–off behavior of pulsed light. Radiant exposure of pulsed light is obtained from total energy divided by the area of the measurement aperture. The measured or calculated radiant exposure of an optical device is compared to the maximum permissible exposure level specified in standards or guidance document for determining the safety level of the device. Some researchers pointed out that the exposure limit in the standard document is lower than the actual damage threshold, thus laser irradiation up to 4 times over the limit will not induce significant injury.[2] Whether over-the-limit exposure will induce actual damage is still under investigation, and while it errs on the side of safety, it could also lead to unnecessarily improper classification of an optical device. As such, accurate determination of the radiant exposure is critical.

Radiant exposure using pulsed source criteria can be measured by the delivered optical energy through a measurement aperture. The maximum radiant exposure of a scanning light through the measurement aperture can be determined by taking the change in dwell-time and overlap into account.[3] However, a spatially stationary but temporally dynamic pulsed light source is physically different from a spatially dynamic but temporally stationary scanning light source. A few studies have explored the different manifestations of pulsed and scanning light sources: overestimated maximum surface temperature when dynamic properties were not considered,[4] increased photodamage when the scanning speed was lowered,[5] and decrease of thermal damage threshold due to multiple exposures from repeated scanning exposures.[6] Systematic studies on the irradiation through a measurement aperture for their physical equivalence have not been reported, to the best of the author's knowledge. Pulsed source analogy has been adapted by some researchers,[7] as has alternative evaluation methods using extended source criteria;[8, 9] these will not be discussed herein.

The main objective of this study is to investigate a new numerical procedure based on the melanin granule model and verify its utility in simulating thermal effects on biological tissue under scanning and pulsed light irradiation through a measurement aperture.

2 Method

A number of theoretical models to describe retinal damage induced by laser pulses have been developed during the past

---

Address all correspondence to: Do-Hyun Kim, Food and Drug Administration, 10903 New Hampshire Ave., Building 62, Room 1133, Silver Spring, Maryland 20993; Tel: 301-796-2609; E-mail: do-hyun.kim@fda.hhs.gov.

decades. For example, a homogeneous layer model successfully addressed the thermal action of laser radiation on ocular tissues.[10,11] However, the homogeneous layer model works well only for a limited range of laser pulses.[12] Melanin granule model (MGM) calculates the temperature change in the tissue assuming that the laser energy is absorbed only by melanosomes.[13] Early versions of the melanin granule model achieved the temperature calculation based on the assumption that the melanosomes are infinitely small. Thompson et al. later extended the model to the finite-sized melanosomes.[12]

Thompson's MGM was adapted for this study for several reasons. First, the model was successfully adapted by many researchers,[14,15] including Schulmeister et al. in their work on the scanning light source problem.[6] A discussion of limitations of MGM in comparison with different numerical models can be found in Thompson's work.[12] Second, the melanin granule model does not involve the rigorous calculation required by other numerical models such as finite difference model (FDM) or finite element model (FEM); rather, the solution to the temperature distribution is given by an ensemble of analytical equations.[12] Simulation of dynamically moving scanning light requires multiple iterations of calculation. FDM and FEM require dynamic change of boundary conditions to calculate the steady-state distribution of temperature in the tissue. Thus, adaptation of FDM or FEM to this study is highly complicated. Cross-validation will be performed in a future study. The complex structure of the retina and retinal damage mechanisms will not be discussed.

Heat diffusion models for moving heat sources have been studied by many researchers; however, rigorous calculation for heat diffusion under scanning laser irradiation has not been reported. In this work, pulsed and scanning light sources will be examined for the respective temperature changes they induce, which are presumed to be manifestations of different dynamic energy diffusion procedures. Thermal damage will be assessed as an Arrhenius rate process. Details of calculations and the relevant parameters are well-defined by Thompson's work,[12] while temperature function $T(r, t)$ was adapted from Carslaw and Jaeger's classic work:[16]

$$T_{r=0}(r, t) = \frac{a^2 A_0}{2\kappa} \left\{ 1 + \left(\frac{2Dt}{a^2} - 1 \right) \text{erf} \left(\frac{a}{2\sqrt{Dt}} \right) \right.$$
$$\left. - 2\sqrt{\frac{Dt}{\pi a^2}} e^{-a^2/4Dt} \right\},$$
(1)

$$T_{0<r<a}(r, t) = \frac{DA_0 t}{\kappa} \left\{ 1 - \frac{2a}{r} i^2 \text{erfc} \left(\frac{a-r}{2\sqrt{Dt}} \right) \right.$$
$$+ \frac{2a}{r} i^2 \text{erfc} \left(\frac{a+r}{2\sqrt{Dt}} \right) - \frac{4\sqrt{Dt}}{r} i^3 \text{erfc} \left(\frac{a-r}{2\sqrt{Dt}} \right)$$
$$\left. + \frac{4\sqrt{Dt}}{r} i^3 \text{erfc} \left(\frac{a+r}{2\sqrt{Dt}} \right) \right\},$$
(2)

$$T_{r\geq a}(r, t) = \frac{2DA_0 ta}{r\kappa} \left\{ i^2 \text{erfc} \left(\frac{r-a}{2\sqrt{Dt}} \right) + i^2 \text{erfc} \left(\frac{r+a}{2\sqrt{Dt}} \right) \right.$$
$$- \frac{2\sqrt{Dt}}{a} i^3 \text{erfc} \left(\frac{r-a}{2\sqrt{Dt}} \right)$$

$$\left. + \frac{2\sqrt{Dt}}{a} i^3 \text{erfc} \left(\frac{r+a}{2\sqrt{Dt}} \right) \right\},$$
(3)

where D is thermal diffusivity, κ is thermal conductivity, a is granule radius, and A_0 is the optical energy production rate calculated by the below relation:

$$A_0 = \frac{3I_0}{4a\tau} \left\{ 1 - \frac{1}{2a^2\alpha_m^2} [1 - e^{-2a\alpha_m}(1 + 2a\alpha_m)] \right\},$$
(4)

where I_0 is the fluence at the retina, α_m is absorption coefficient of melanosome, and τ is the pulse duration. Error function and its derivatives in Eqs. (1)–(3) are given as:

$$\text{erfc}(x) = 1 - \text{erf}(x) = \frac{2}{\sqrt{\pi}} \int_x^\infty e^{-\eta^2} d\eta,$$
(5)

$$i^2 \text{erfc}(x) = \frac{1}{4} \left[(1 + 2x^2) \text{erfc}(x) - \frac{2}{\sqrt{\pi}} x e^{-x^2} \right],$$
(6)

$$i^3 \text{erfc}(x) = \frac{1}{6} \left[\frac{1}{\sqrt{\pi}} e^{-x^2} - x \text{erfc}(x) - 2x i^2 \text{erfc}(x) \right].$$
(7)

Temperature at different position (r) and time (t) can be calculated using Eqs. (1)–(7). When $t > \tau$, the representation for the temperature becomes:

$$T^*(r, t > \tau) = T(r, t) - T(r, t - \tau).$$
(8)

All the numerical analyses were performed using an open-source software (Octave, GNU). Calculation results for temperatures at different locations, times, and pulse durations were validated by comparing with other researchers' results.[12,17]

The MGM in general is implemented using the random positioning of melanosomes in the retinal layer as shown in Fig. 1(a). This random distribution of melanosomes resembles the real retinal tissue structure. In MGM, laser radiant exposure at each melanosome should be calculated by subtracting the portion of light energy absorbed and scattered by melanosomes in upper layers, when the light is illuminated from the top. Melanosomes typically are 1 to 2 μm in diameter and are randomly distributed in whole retinal pigment epithelium (RPE) layer. Random distribution of melanosomes can induce anisotropic distribution of temperature change. An exaggerated distribution of melanosomes that exhibit large anisotropy in temperature calculation is shown in Fig. 1(a). A mathematical method to avoid this error is to average the results from multiple calculations. Each
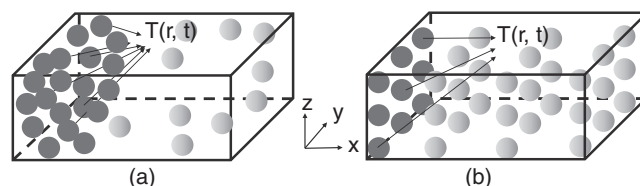
Fig. 1 Illustration of melanin granule model: (a) melanosomes are randomly distributed in the retinal layer in traditional model. This example shows an exaggeratedly non-uniform distribution of melanosomes; (b) melanosomes are uniformly distributed in the retinal layer mimicking the lattice structure. Light illumination is from positive-z direction. Melanosomes being irradiated are shaded.

calculation is independent of all others, thus the norm of the temperature will obey a Gaussian distribution. Another simplified method of avoiding this error from random distribution is to eliminate the randomness itself. If melanosomes are positioned in RPE uniformly, as shown in Fig. 1(b), anisotropic contribution to the temperature is eliminated. Uniformly distributed MGM has been successfully adapted by other authors.[15] This uniform distribution of melanosomes is highly effective for revealing the differences between spatially stationary pulsed light and spatially dynamic scanning light.

A new computational procedure is developed based on the uniform MGM. Since the uniform distribution of melanosomes resembles the crystal lattice structure in solid state physics, the computational model is named melanin granule lattice model (MGLM). The RPE layer with uniformly distributed melanosomes can be assigned with a tetragonal lattice, which contains one melanosome in one unit-cell. All the melanosomes in the whole volume can be addressed by integer multiples of unit-vector, thus, the computational procedure can be simplified to three nested repetition-loops (in the x, y, and z directions) without using any Boolean procedures. When the temperature $T(r, t)$ is calculated at the position r in the top layer, the difference in z-position of melanosomes of different layers only contributes as different magnitude of temperature increase in $T(r, t)$. Their contributions from different y-positions are symmetric about the x-z plane. Only the difference in their x-positions will reflect the effect from spatial dynamic change of pulsed or scanning light. MGLM enables the sequential calculation of thermal contribution from individual melanosomes in simplified computational procedure, which is an advantage for studying scanning light irradiation.

3 Calculation Details

Parameters for temperature calculations were summarized in Table 1.[12,15,17] The radiant exposure at the cornea (I_c) was set to 10 μJ/cm^2, and the retinal radiant exposure (I_0) was approximated by multiplying I_c by a factor of 10^5.[12] This factor is due to the reduced beam spot size at the retina caused by the focusing of the cornea and the lens. Thermal diffusivity (D) can be calculated by $\kappa/\rho c_p$. Melanosome radius (a) was 1.0 μm (Ref. 12) and the melanosomes were distributed in square lattice unit-cell

Table 1 Summary of parameters for calculation.

Variable	Symbol	Value
Thermal conductivity	κ	5.0323×10^{-3} J/cm/K/s
Tissue density	ρ	1.0 g/cm^3
Melanosome radius	a	1 μm
Heat capacity	c_p	4.186 J/g/K
Melanin absorption coefficient	α_m	2000/cm
Frequency factor	lnA	228.22
Activation energy	E_a	627.6 kJ/mole
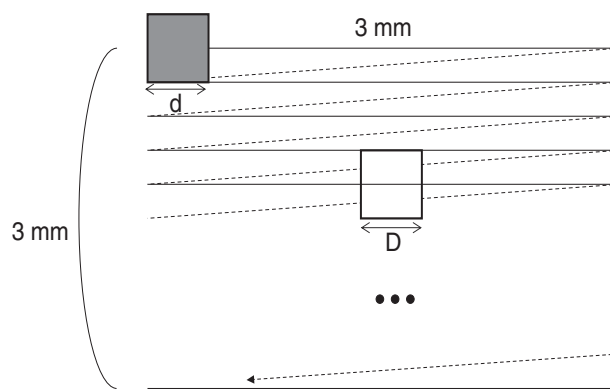
Fig. 2 Illustration of scanning pattern used for the numerical simulation. Empty square represents the measurement aperture and the shaded square represents the laser spot.

without a gap between them.[15] Melanin absorption coefficient (α_m) ranges from 500 to 4000/cm. In this study, α_m was adapted from Thompson's work for 532 nm light sources.[12]

ISO 15004-2 specifies that irradiation will be measured for the localized radiant power that is incident upon a circular area on the retina with a diameter of 180 μm for a nonstabilized eye and 30 μm for a stabilized eye. For a laser that produces a scanning laser beam pattern on the retina, this means that the radiant energy in the beam must be collected and summed each time the beam passes over the specified circular area in a stationary position on the retina for a complete diagnostic procedure or multiple procedures. The main objective of this study is to verify the temperature difference induced by the pulsed and scanning lights when the radiant exposure is measured through a measurement aperture, thus multiple exposures will not be considered. A scanning pattern and a measurement aperture that provides sufficient information to achieve the objective were designed as follows.

Figure 2 shows a saw-tooth scanning pattern that simulates a realistic scanning laser device, such as scanning laser ophthalmoscope. For simplicity of the calculation, laser spot (size $= d$) and the measurement aperture (size $= D$) were assumed to be the same (30 μm). Laser spot of this size is the minimal visible lesion size observed from nonhuman primate eyes.[18] Without adaptive optics, the laser spot size at human retina is about 10 to 20 μm and the typical scanning area is 9 to 16 mm^2 (Ref. 19). For higher image quality, a 50% overlap between two adjacent scanning lines was assumed. For a scanning laser spot to cover 3 mm × 3 mm scanning area, the y- and x-axis scanning frequencies should be 1 and 200 Hz, respectively. The scanning system will produce 200 pixels ×200 pixels of an image at 1 frame/s acquisition rate. The x-axis scanning mirror returns to the scan-origin almost instantaneously with saw-tooth signal, thus the x-axis speed (v_x) of the laser movement is 0.6 m/s ($= 3$mm × 200 Hz).

Determination of dwell-time (τ) seems straightforward when a linearly scanning beam with constant scanning speed (v) is moving over an aperture with size D. A common mistake is to use $\tau = D/v$ without considering the spot size. The dwell-time should be measured from the moment when the right edge of the laser spot starts to appear at the left edge of the aperture until it fully disappears from the aperture. Thus the dwell-time will be
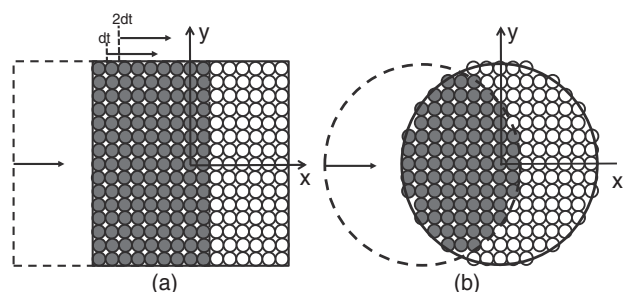
Fig. 3 Illustration of detail of melanosomes involved in the temperature calculation for (a) square and (b) circular laser spot and measurement aperture. Solid and dashed boundary lines represent the measurement aperture and the laser spot, respectively. Melanosomes being irradiated are shaded.

expressed as:

$$\tau = (D + d)/v. \tag{9}$$

For the scanning model shown in Fig. 2, τ is 100 μsec. MGM results agree well with FDM for pulse duration longer than 10 μsec,[15] thus this particular scanning system is a valid example. The MGM cannot calculate temperature from partially irradiated melanosome. It is assumed that the first column of melanosomes starts to be irradiated at full intensity when the laser enters the melanosome site, and then the second column of melanosomes starts to be irradiated after a time interval dt, where dt is 3.3 μsec ($= 2a/v$).

Figure 3(a) illustrates the melanosomes involved in the calculation process for the square laser spot and the aperture. The scanning is in the x-direction and the measurement aperture is centered at the origin of the x-y plane. The first column of melanosomes starts to be irradiated when the laser spot enters into the aperture from the left, and the irradiation continues until the left edge of the laser spot departs the first column. The time duration is d/v ($= \tau/2$ in this example). After dt, the second column starts to be irradiated and it also continues to be irradiated for $\tau/2$. The process repeats until the entire laser spot passes through the aperture. The temperature change at $r(x, y, z)$ contributed by all the melanosomes inside the measurement aperture will be calculated using MGLM at time T after the laser irradiation is completed. $T(r, t)$ and T are not to be confused. All the spatial laser profiles are top-hat. The temporal intensity change measured through the aperture actually is triangular; however, a step-function pulse will be used for two reasons: First, the time duration each melanosome is irradiated is the same ($\tau/2$) for all melanosomes, which resembles step-function pulse irradiation; Second, MGM works well for step-function irradiation. Triangular or Gaussian temporal profiles will be studied in the future.

Figure 3(b) illustrates the calculation details for the circular laser spot and the measurement aperture. The major difference of circular geometry from square geometry is that each melanosome starts to be irradiated at different time and for different time duration. Melanosomes on the x-axis are irradiated for the longest time duration ($\tau/2$), while those near the upper and bottom edge of the aperture are irradiated for a shorter time duration. Pulsed laser irradiates all the melanosomes for the same time duration. Melanosomes outside of aperture are not considered because consideration of all melanosomes is ade-

quate for extended source criteria, not for pulsed source criteria where scanning lights are treated as pulsed lights. This analogy is based upon the usage of the measurement aperture, which restricts the exposure of the light source to a limited area under the open aperture.

4 Results

A series of numerical calculations have been performed to obtain the temperature and thermal damage threshold at a position (x, y, z) at time T after the irradiation. Nominal thickness of the RPE layer is 10 to 15 μm,[20] within which 5 monolayers of melanosomes were placed for calculation. An MGM calculation shows discrepancy between the temperatures inside and outside of melanosome during the irradiation ($T = 0$), thus a number of different T's were tested to find calculation results with which the discrepancy was minimal. The results in Secs. 4.1–4.3 were obtained with thus carefully chosen T. The top layer receives full radiant exposure (thus, I_c), while it is attenuated in other layers according to Beer–Lambert's law.[12,17] Intensity at the second layer is reduced by $\exp(-2\alpha_m a)$, and by $\exp(-8\alpha_m a)$ for the bottom layer. As explained in Sec. 3, the dwell-time for the scanning laser is τ ($= 100$ μsec), and the same τ is used as the pulse duration. The calculation results for temperatures using melanin granule model are temperature changes, not the absolute temperature. Only a single line of scan was considered in this study to investigate the difference between pulsed and scanning light sources. Calculation results in square geometry for temperature changes and thermal damage threshold will be discussed in Secs. 4.1 and 4.2, respectively. In Sec. 4.3, temperature calculation in circular geometry will be briefly discussed.

4.1 Temperature Changes in Square Geometry

Figure 4 shows the calculation results for the square geometry at $T = 10$ μsec and $y = z = 0$. The maximum temperature rise at $t (= T + \tau)$ after the first irradiation start (T after the irradiation completion) was 94.4 K for the scanning laser. As was explained in Sec. 3, actual irradiation time for each melanosome is $\tau/2$.
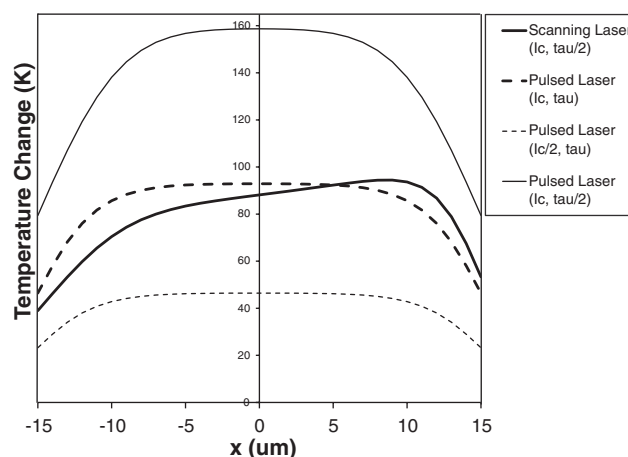
Fig. 4 Calculation results for square laser and aperture: $T = 10$ μsec; $y = z = 0$. For the pulsed laser, different radiant exposures (I_c and $I_c/2$) and pulse durations (τ and $\tau/2$) were used. $I_c = 10$ μJ/cm^2, and $\tau = 100$ μsec.
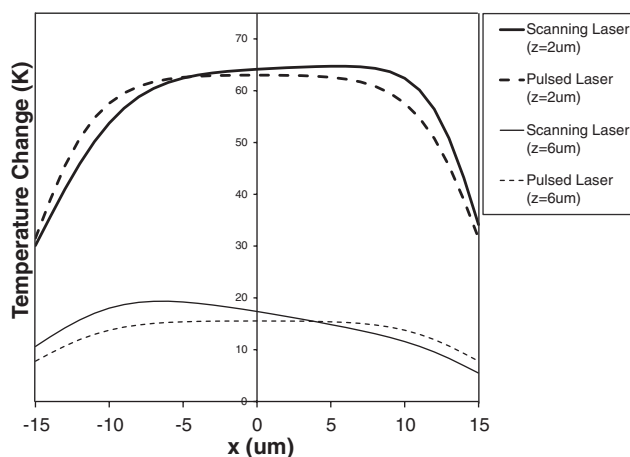
Fig. 5 Calculation results for square scanning and pulsed lasers with different measurement z-coordinates ($z = 2$ μm and 6 μm). $I_c = 10$ μJ/cm^2, $\tau = 100$ μsec, and $T = 10$ μsec.

Fig. 6 Calculation results for square scanning laser with different measurement time ($T = 0$, 10, 100, and 200 μsec). $I_c = 10$ μJ/cm^2, $\tau = 100$ μsec, and $z = 0$.

The maximum temperature rise was 158.3 K for the pulsed laser with radiant exposure I_c and pulse duration $\tau/2$, which was significantly higher than that of the scanning laser. Calculating the pulse duration by dividing the aperture diameter by the scanning speed (D/v) is common mistake when evaluating the scanning laser using pulsed source criteria. As the temperature calculation results showed, temperature change includes a great error if D/v is used as the dwell-time for the scanning laser.

Another way to estimate the laser pulse parameter is to compare actual laser energy delivered through the aperture. Melanosomes were irradiated for the time duration $\tau/2$ by the laser radiant exposure (I_c). For a pulsed laser to deliver the same amount of laser energy to each melanosomes during the time duration τ, a laser with half the radiant exposure ($I_c/2$) should be used. The calculation result for a pulsed laser with $I_c/2$ is also shown in Fig. 4. The maximum temperature rise was 46.4 K, which was much lower than the previous results. These two examples suggest that calculating the dwell-time for a scanning laser using Eq. (9) might be the proper way. When the pulse duration of the pulsed laser was set to the dwell-time of the scanning laser (τ), the maximum temperature rise was 92.8 K for the pulsed laser with full laser intensity (I_c). Although scanning laser produced a slightly higher temperature rise, the difference was smaller than the previous examples. These results suggest that the thermal effect of a scanning laser is different from that of a pulsed laser. These results also suggest that equivalent pulse duration for scanning laser is $(D + d)/v$ rather than D/v. Pulse duration τ and full radiant exposure I_c will be used for pulsed lasers in the following temperature calculations.

Figure 5 shows the calculation results for lasers with $\tau = 100$ μsec and $T = 10$ μsec, at different z-positions. The maximum temperature rises were 63.0 and 64.6 K at $z = 2$ μm for pulsed and scanning laser, respectively. As z increased, the temperature change decreased: 15.5 and 19.3 K at $z = 6$ μm for pulsed and scanning laser, respectively. The maximum temperature occurred at $x = 7$ μm when $z = 2$ μm, however, it shifted to $x = -6$ μm when $z = 6$ μm. These shifts of peak temperature position are believed to be related to the heat diffusion process, and will be discussed in Sec. 4.2. The temperature difference between pulsed and scanning laser at $z = 2$ μm was 1.6 K,
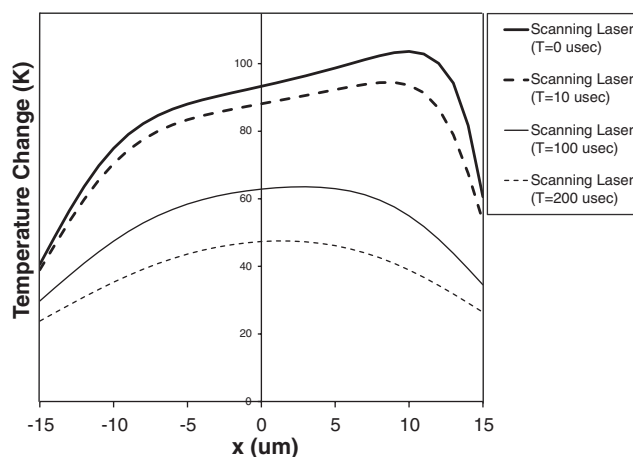
however, it was 3.8 K at $z = 6$ μm. These results imply that the difference in thermal process of scanning and pulsed laser is not uniform in the entire retinal layer.

Figure 6 shows the calculation results at $z = 0$ with varying time T (0, 10, 100, and 200 μsec). As was in the case for varying z, similar peak shifts were observed. The peak temperatures were 103.6, 94.4, 63.4, and 47.5 K for $T = 0$, 10, 100, and 200 μsec, respectively. The x-position of peak temperature shifted from positive to negative. The larger T provides enough time for the heat to be dissipated into the broader tissue area, thus the temperature distribution from a scanning laser resembles that from a pulsed laser.

Figure 7 shows the calculation results for different scanning speeds. The scanning speed for the previous results is for a 200×200 pixels image ($v = 0.6$ m/s), while Fig. 7 shows the results for 100×100 pixels ($v = 0.3$ m/s) and 500×500 pixels ($v = 1.5$ m/s). The scanning speeds of $v = 0.3$ m/s and $v = 1.5$ m/s correspond to the dwell-time (τ) of 200 and 40 μsec, respectively. MGM results for a dwell-time shorter than 10 μsec is not comparable to FDM results,[15] and a dwell-
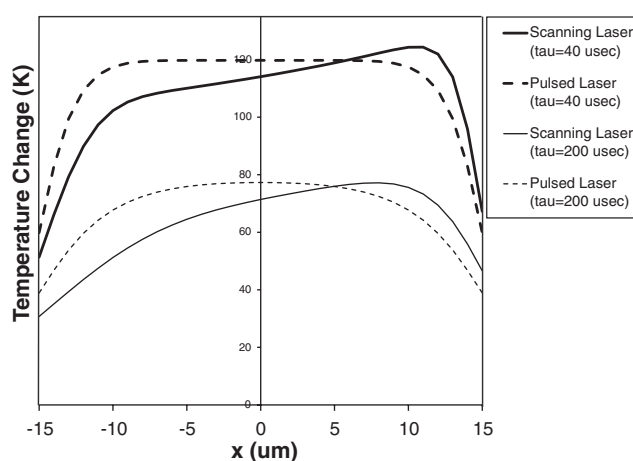
Fig. 7 Calculation results for square scanning and pulsed laser with different dwell-time ($\tau = 40$ and 200 μsec), $z = 0$ μm.

time longer than 200 μsec does not provide a realistic image speed, thus the given results for 40 to 200 μsec are useful. Combined with the results for $\tau = 100 \mu$sec shown in Fig. 5, maximum temperatures and peak positions have been observed as such: Maximum temperature rises were 119.7, 92.8, and 77.3 K at $x = 0$ for $\tau = 40$, 100, and 200 μsec, respectively; they were 124.3, 94.4, and 76.8 K for $\tau = 40$, 100, and 200 μsec, respectively. The peaks shifted toward the left, which is due to the fact that the longer dwell-time provides enough time for the heat to be dissipated in the tissue.

4.2 Thermal Damage Thresholds in Square Geometry

The temperature calculated at a certain time frame (T) may or may not indicate actual thermal damage to the tissue, thus further investigation is needed. The Arrhenius integral has successfully been used to model tissue damage by many researchers.[10,11] The Arrhenius integral is given as:

$$\Omega(t) = A \int_0^\tau \exp\left[-\frac{E_a}{RT(t)}\right] dt, \qquad (10)$$

where A is the frequency factor, E_a is the activation energy, τ is the pulse duration, $T(t)$ is the temperature in Kelvin, and R is the gas constant (8.31 J/molK). The values for A and E_a are given in Table 1.[21] Analytical calculation of Eq. (10) is not practically possible due to the complex procedure for calculating $T(t)$. A commonly adapted numerical integration method using the trapezoidal rule was adapted for the calculation. Pulse duration (τ) was divided into 30 steps (melanosome irradiation steps), and then the temperature calculated by MGLM above the body temperature (310 K) was used as $T(t)$ in Eq. (10). The minimum radiant exposure for any location in the x-y plane at which Arrhenius integral started to exceed unity is the threshold exposure. Because MGLM calculation produces error for the temperature inside the melanosome during the irradiation, results for $z > 0$ and $T = 10 \mu$sec were obtained. Integration in Eq. (10) was repeatedly performed over the tissue area inside the measurement aperture in 30 steps using different values of I_c in Eqs. (1)–(7) until it exceeded unity.

Table 2 summarizes the calculated threshold exposures for $z = 2$, 4, and 6 μm; and for $\tau = 40$, 100, and 200 μsec. Corresponding temperatures are shown in Figs. 5 and 7, respectively. When τ was fixed at 100 μsec, threshold exposure was slightly lower for the pulsed laser at $z = 2 \mu$m; however, it was lower by 17.6% for the scanning laser at $z = 6 \mu$m. This is believed to be due to the different heat diffusion characteristics from pulsed and scanning lasers. A location in the tissue further away from the melanosome layers receives well diffused thermal energy from moving (scanning) laser, thus the thermal contribution from the beginning of scanning laser in the aperture plays more role to the thermal damage. The threshold for scanning laser was lower for $\tau = 40 \mu$sec while it reversed at $\tau = 200 \mu$sec. The calculation results showed that there exists a difference in damage threshold, while the difference was not significantly large for different pulse durations.

Table 2 Calculation results of damage threshold radiant exposure.

	Threshold I_c pulsed laser	Threshold I_c scanning laser
$\tau = 100 \mu$sec		
$z = 2 \mu$m	0.551×10^{-5} J/cm^2	0.553×10^{-5} J/cm^2
$z = 4 \mu$m	1.14×10^{-5} J/cm^2	1.10×10^{-5} J/cm^2
$z = 6 \mu$m	2.54×10^{-5} J/cm^2	2.10×10^{-5} J/cm^2
$z = 2 \mu$m		
$\tau = 40 \mu$sec	0.586×10^{-5} J/cm^2	0.581×10^{-5} J/cm^2
$\tau = 100 \mu$sec	0.551×10^{-5} J/cm^2	0.553×10^{-5} J/cm^2
$\tau = 200 \mu$sec	0.541×10^{-5} J/cm^2	0.544×10^{-5} J/cm^2

4.3 Circular Geometry

Square-shaped laser spot and measurement aperture are not commonly used. However, the purpose of using square geometry in Secs. 4.1 and 4.2 was not only for its simplicity in numerical calculation. Each melanosome inside the measurement aperture receives the same amount of laser energy when the laser and aperture are both square, thus estimating pulse parameters is straightforward for square geometry. Nevertheless, it is necessary to investigate more practical circular laser spot and circular aperture. Figure 8 shows the calculation results for circular geometry, both with 30 μm in diameter. The calculation procedure is significantly more complicated compared to the square geometry. The biggest difference is that each melanosome takes laser irradiation for different time duration. Figure 8 shows temperature profile on the x-axis, ($y = 0$, $z = 0 \mu$m) for pulse lasers with different radiant exposure (I_c, $I_c/2$, and $I_c/3$). Temperature rise from a scanning laser was much lower than that from a pulsed laser. The peak temperature from a scanning laser was lower than that of a pulsed laser with 33% radiant exposure. This study suggests that the exposure from a circular scanning laser will
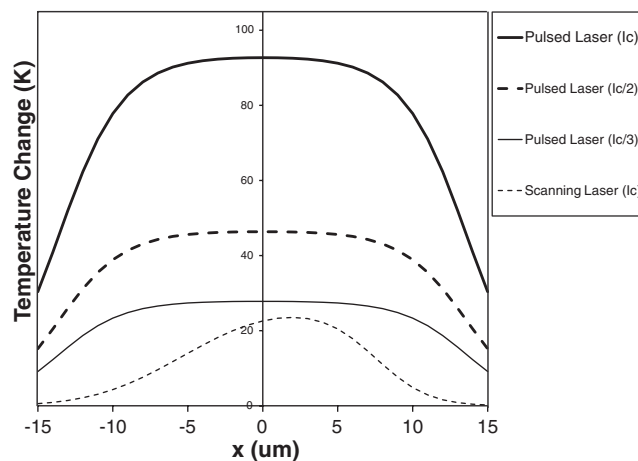
Fig. 8 Calculation results for circular laser and measurement aperture for pulsed lasers with different intensity (I_c, $I_c/2$, and $I_c/3$) and a scanning laser.

be underestimated when it was evaluated by the pulsed-source criteria using a measurement aperture with a similar aperture size. If the laser spot size is significantly larger than the aperture size ($d \gg D$), or vice versa ($d \ll D$), both the square and circular geometries will produce similar results.

5 Discussion

The calculation results confirmed that the dynamic procedure of temperature changes in pigmented retinal layer is different for pulsed and scanning exposures. Two types of exposures delivered exactly the same amount of light energies through the measurement aperture, and the differences in maximum temperature between pulsed and scanning light irradiations were not significantly large for the tissue and laser parameters used for this study. However, it is confirmed that the spatial distribution of the temperature and the maximum temperature change are not equal. As can be seen from Figs. 4–7, the local temperature maxima from scanning light sources were shifted away from the mid-point of measurement aperture, suggesting that the thermal effect at a certain location of the tissue was affected by the heat diffused from formerly irradiated cells (melanosomes) under a moving light source. Evaluation of a scanning light source using pulsed source criteria with a measurement aperture does not fully incorporate this effect, suggesting that the entire tissue area under light irradiation must be considered for the evaluation of scanning light sources.

For optical radiation hazard evaluation, overestimation of thermal effect gives a larger margin in the maximum permissible exposure, which is beneficial to the safety of a biological specimen under laser exposure. However, safety is not the only factor that governs the successful function of optical medical devices. Excessively suppressed optical output level from optical medical devices often leads to the degradation of the effectiveness; thus, a proper balance between the safety and effectiveness is essential. For underestimated exposures, pulse duration needs to be adjusted to increase safety, while the reverse is needed for overestimated exposures in terms of optimal effectiveness. The results presented here demonstrate the temperature change and thermal damage threshold within measurement apertures, which suggest that evaluating scanning laser exposure by pulsed laser criteria is not scientifically exact. As such, additional scrutiny is needed which perhaps expands upon the MGLM model introduced here. Future work should consider global temperature change and thermal effects for the entire specimen under scanning laser exposure. Comparison with other numerical methods such as FDM and FEM will also provide valuable information.

6 Conclusion

The difference in temperature change and thermal damage threshold in the pigmented retinal layer under pulsed and scanning light sources within the measurement aperture was numerically studied for the first time. Using the calculation parameters and formulation of MGM, a simple and effective calculation model, MGLM was implemented. MGLM was proved to be useful for calculating temperature changes and damage thresholds from scanning and pulsed light sources. MGLM provides a simplified computational procedure in calculating sequential temperature changes and thermal damage thresholds contributed by individual melanosomes or individual columns of melanosomes. When equivalent pulse duration and dwell-time for pulsed and scanning lasers are used, a laser irradiation through a measurement aperture produced slightly different temperature rise and thermal damage threshold for a scanning laser compared to a pulsed laser. The calculation also revealed that equivalent pulse duration for scanning laser is $(D + d)/v$ rather than D/v. Finding proper pulse parameters is important because error in determination of irradiation level will lead to improper classification of optical devices. This study suggests that current evaluation methods of scanning light source based on pulsed source criteria can be used if equivalent pulse parameters are properly determined. However, this study also suggests that further study is required to establish a thorough and complete evaluation method of scanning light sources for their optical radiation hazard.

References

1. ISO 15004-2: International Standard for ophthalmic instruments and for light hazard protection, Part 2 (2007).
2. D. H. Sliney, "Ocular radiation Hhzards," in *Handbook of Optics*, M. Bass, Ed., Optical Society of America and McGraw-Hill, New York (2000).
3. D.-H. Kim, "Evaluation of phototoxicity from scanning biophotonic devices," presented at SPIE Photonics West, San Francisco, California, January 22–28, 2011.
4. K. M. McNally, A. E. Parker, D. L. Heintzelman, B. S. Sorg, J. M. Dawes, T. J. Pfefer, and A. J. Welch, "Dynamic optical-thermal modelling of laser tissue soldering with a scanning source," *IEEE Sel. Top. Quant. Electron* **5**(4), 1072–1082 (1999).
5. C. Framme, C. Alt, S. Schnell, M. Sherwood, R. Brinkmann, and C. P. Lin, "Selective targeting of the retinal pigment epithelium in rabbit eyes with a scanning laser beam," *Invest. Ophthalmol. Visual Sci.* **48**(4), 1782–1792 (2007).
6. K. Schulmeister, R. Gilber, B. Seiser, F. Edthofer, J. Husinsky, B. Fekete, and L. Farmer, "Retinal thermal laser damage thresholds for different beam profiles and scanned exposure," *Proc. SPIE* **6844**, 68441L (2008).
7. W. T. J. Ham, H. A. Mueller, M. L Wolbarsht, and D. H. Sliney, "Evaluation of retinal exposures from repetitively pulsed and scanning lasers," *Health Phys.* **54**, 337–344 (1988).
8. L. Li and J. S. Rosenshein, "Safety considerations for simultaneous multiple wavelength exposure in scanning laser ophthalmoscopes," *Health Phys.* **64**, 170–177 (1993).
9. U. Klingbeil, "Safety aspects of laser scanning ophthalmoscopes," *Health Phys.* **51**, 81–93 (1986).
10. A. J. Welch, "The thermal response of laser irradiated tissue," *IEEE J. Quant. Electron.* **QE-20**, 1471–1482 (1984).
11. R. Birngruber, F. H. Hillenkamp, and V. P. Gabel, "Theoretical investigation of laser thermal retinal injury," *Health Phys.* **48**, 781–796 (1985).
12. C. R. Thompson, B. S. Gerstman, S. L. Jacques, and M. E. Rogers, "Melanin granule model for laser-induced thermal damage in the retina," *Bull. Math. Biol.* **58**(3), 513–553 (1996).
13. W. P. Hansen and S. Fine, "Melanin granule models for pulsed laser induced retinal injury," *Appl. Opt.* **7**(1), 155–159 (1968).
14. V. K. Pustovalov and B. Jean, "Melanin granule models for the processes of laser-induced thermal damage in pigmented retinal tissues. I.

Modeling of laser-induced heating of melanosomes and selective thermal processes in retinal tissues," *Bull. Math. Biol.* **69**, 245–263 (2007).

15. K. Schulmeister, J. Husinsky, B. Seiser, F. Edthofer, B. Fekete, L. Farmer, and D. J. Lund, "Ex vivo and computer model study on retinal thermal laser-induced damage in the visible wavelength range," *J. Biomed. Opt.* **13**(5), 054038 (2008).

16. H. S. Carslaw and J. C. Jaeger, *Conduction of Heat in Solids*, Chap. 13, Clarendon Press, Oxford, London (1947).

17. K. Schulmeister, ARC Seibersdorf Research, 2444 Seibersdorf, Austria, personal communication (2011).

18. B. J. Lund, D. J. Lund, and P. R. Esdall, "Laser-induced retinal damage threshold measurements with wavefront correction," *J. Biomed. Opt.* **13**(6), 064011 (2008).

19. P. F. Sharp and A. Manivannan, "The scanning laser ophthalmoscope," *Phys. Med. Biol.* **42**, 951–966 (1997).

20. M. Shakib and K. M. Zinn, "Fine structure and function of ocular tissues. The choroid, Bruch's membrane, and the retinal pigment epithelium," *Int. Ophthalmol. Clin.* **13**, 189–204 (1973).

21. A. J. Welch and G. D. Polhamus, "Measurement and prediction of thermal injury to the retina of the Rhesus monkey," *IEEE Trans. Biomed. Eng.* **BME-31**(10), 633–643 (1984).